

Isotopic evaluation of the National Water Model reveals missing agricultural irrigation contributions to streamflow across the western United States

Annie L. Putman¹, Patrick C. Longley², Morgan C. McDonnell¹, James Reddy³, Michelle Katoski⁴, Olivia L. Miller¹, and J. Renée Brooks⁵

¹US Geological Survey Utah Water Science Center

²US Geological Survey Colorado Water Science Center

³US Geological Survey New York Water Science Center

⁴US Geological Survey Maryland-Delaware Water Science Center

⁵US Environmental Protection Agency, Pacific Ecological Systems Division

Correspondence: Annie L. Putman (aputman@usgs.gov)

Abstract. The National Water Model (NWM) provides critical analyses and projections of streamflow that support water management decisions. However, the NWM performs poorly in lower elevation rivers of the western United States (US). The accuracy of the NWM depends on the fidelity of the model inputs and the representation and calibration of model processes and water sources. To evaluate the NWM performance in the western US, we compared observations of river water isotope ratios ($^{18}O/^{16}O$ and $^2H/^1H$ expressed in δ notation) to NWM-flux-estimated (model) river reach isotope ratios. The modeled estimates were calculated from long term (2000-2019) mean summer (JJA) NWM hydrologic fluxes and gridded isotope ratios using a mass balance approach. The observational dataset comprised 4503 in-stream water isotope observations in 877 reaches across 5 basins. A simple regression between observed and modeled isotope ratios explained 57.9% ($\delta^{18}O$) and 67.1% (δ^2H) of variance, though observations were 0.5‰ ($\delta^{18}O$) and 4.8‰ (δ^2H) higher, on average, than mass balance estimates. The unexplained variance suggest that the NWM does not include all relevant water fluxes to rivers. To infer possible missing water fluxes, we evaluated patterns in observation-model differences using $\delta^{18}O_{diff}$ ($\delta^{18}O_{obs} - \delta^{18}O_{mod}$) and d_{diff} ($\delta^2H_{diff} - 8 * \delta^{18}O_{diff}$). We detected evidence of evaporation in observations but not model estimates (negative d_{diff} and positive $\delta^{18}O_{diff}$) at lower elevation, higher stream order, arid sites. The catchment actual evaporation to precipitation ratio, the fraction of streamflow estimated to be derived from agricultural irrigation, and whether a site was reservoir-affected were all significant predictors of d_{diff} in a linear mixed effects model, with up to 15.2% of variance explained by fixed effects. This finding is supported by [patterns in seasonal patterns as well as](#) groundwater levels and [groundwater](#)-isotope ratios, and suggests the importance of including irrigation return flows to rivers, especially in lower elevation, higher stream order, arid rivers of the Western US.

20 1 Introduction

The western United States (US) is experiencing multidecadal drought ? and declining streamflows ?. Major rivers are running dry ?, lakes are shrinking ???, and water users are experiencing shortages and cuts ?. These decreases in streamflow and groundwater fluxes are projected to continue in coming years ??, with projected decreases in snowpack ?? and increases in temperatures ?. Under drought and snow drought stress, as well as changing wintertime precipitation patterns, river flows may become more difficult to forecast ??. Yet, with decreasing water availability, water managers and other stakeholders tasked with managing and responding to current and future water supply increasingly depend on accurate streamflow predictions.

Fully routed, high spatial and temporal resolution streamflow models, like the National Oceanic and Atmospheric Administration's National Water Model (NWM) which is an application of the Weather Research and Forecasting (WRF) Hydro model ?, provide short and medium term streamflow prediction in the United States, as well as analyses of past stream discharge at ungaged locations. The accurate, detailed, frequent results from the National Water Model may be used by emergency managers, reservoir operators, floodplain managers, and farmers to aid in water use decision making and flood or pollution risk evaluation. The accuracy of predictions and current snapshots produced by the model depend on 1) inclusion and faithful representation of relevant water sources and hydrologic processes 2) appropriate calibration of parameter estimations and 2) the fidelity of the model inputs.

With respect to the faithful representation of water sources, the major water sources to streams in the mountainous west include two broad water flux categories: runoff (also called quickflow, and may comprise surface or subsurface waters) and groundwater discharge (also called baseflow). Runoff during the summer comes from late season snowmelt, rain, and irrigation water. Groundwater discharge comes from shallow or deep in-ground water, typically recharged at high elevation by snowmelt. Rivers in the west derive the majority of their water from spring-time melt of high elevation wintertime snowpack ?? and little water is contributed to streams at lower elevations where there is minimal snowpack ?. Some of the melt water enters streams as surface runoff during late spring and summer, while the remainder recharges shallow and deep groundwater and later in the season or in subsequent years enters the stream as groundwater discharge ?????. Rain contributes runoff to streamflow, but even in areas receiving a substantial proportion of their total annual precipitation during summer in association with the North American Monsoon, only a small proportion of the total precipitation makes it to the stream ??; ~~the remainder~~ most is evaporated from soils or transpired by plants ?. Thus, lower elevation streams, particularly later in the summer, depend heavily on groundwater discharge from higher elevations to sustain their flows ? and the majority of streams in lower elevation arid areas are likely to lose water to shallow groundwater recharge ?.

Within this hydrologic framework, human water use and management introduces complexity via reservoirs and managed release schedules, trans- and interbasin transfers, conveyances, and surface and groundwater withdrawals, as well as irrigation for agricultural crop or turf grass growth. Turf irrigation in cities composes the majority of household water use in most municipalities and agricultural irrigation can comprise up to 80% of total statewide water use in

Western US states ?. Water used for agricultural crop or turf grass growth locally intensifies water balance fluxes, through increases in both water application and evapotranspiration in these select tracts of land. Depending on the method, both agriculture and turf grass irrigation can contribute to local groundwater recharge ?, with greater recharge coming from flood irrigation compared to sprinkler or drip irrigation methods. Water for irrigation can come from either surface or groundwater withdrawals. The irrigation water source may have both direct and indirect influences on streamflows particularly during low flow seasons, and may, depending on conditions, may contribute to streamflow increases, decreases, or delays in discharge ????. However, these processes and fluxes are not currently explicitly included in the NWM.

Past NWM evaluations have leveraged streamgage measurements ~~???~~ ~~???~~ and model evaluation using streamgage measurements is included in the NWM WRF-Hydro workflow ?. Using measured discharge to evaluate the NWM is useful because the data are publicly available at high spatial and temporal resolution (e.g., dataset used in ?). However, evaluation of streamflows with measured discharge 1) may allow modelers to get the correct total streamflow values and temporal patterns at a reach for the wrong process reasons or 2) may suggest that the model could be improved due to mismatches between measured and modeled data, but cannot provide information on the specific process(es) or sources responsible for the errors.

Among the climatic regions covered by the NWM, model streamflow evaluation metrics perform the most poorly in the Western US in lower elevation reaches. Metrics like the Kling-Gupta efficiency (KGE) indicate pervasive mismatches between measured and modeled streamflows and percent bias (PBIAS) results showed that simulated streamflow volumes tend to be overestimated in the west ?. Similarly, ? found that the NWM has difficulty estimating flows during drought or low flow years in the Colorado River Basin. In the low elevation stream reaches of the Western US, disagreement between the NWM flows and observations within anthropogenically-altered reaches may come from incomplete representation of anthropogenic water sources or processes in the NWM.

In the western US, low elevation waterways have moderate to high potential for anthropogenic alteration ?. ~~For example, rivers~~ Rivers and surface water supplies are managed by dams, and a large proportion of total water use is allocated to irrigating agriculture ?. However, the NWM does not explicitly include surface water removal for agricultural irrigation nor subsurface return flows from irrigation in its streamflow computations. Likewise, the NWM represents inflow and outflow of lakes and reservoirs as passive storage and releases, with no active reservoir management. Both of these omissions may be contributors to the large errors observed in the NWM in lower elevation areas where land use includes large amounts of along-river agriculture and streamflow is heavily managed through reservoir operations. Unfortunately, the effects of contributions of these two water sources on streamflow are difficult to identify and quantify through evaluations of streamflow records alone.

Elemental or isotope ratios in media associated with hydrologic processes (i.e., water, dissolved gasses, suspended sediments, dissolved ions) are used used to track the contributions of specific water sources (e.g., groundwater, runoff) to rivers or other surface waters ????. Tracers are useful because they provide information that is otherwise impossible to disentangle from direct measurements of streamflow.

Stable water isotopes (~~H and O~~ O and H) have been used to extract hydrologic process information ?? and diagnose
90 process limitations in other modeling contexts ?. Water comprises three commonly measured stable isotopologues:
the most abundant, light atom-bearing $^1H_2^{16}O$, as well as ~~a heavy hydrogen bearing ($^1H^2H^{16}O$) and a heavy-heavy~~
oxygen bearing (~~$^1H_2^{18}O$~~ $^1H_2^{18}O$) ~~and heavy hydrogen bearing ($^1H^2H^{16}O$)~~ isotopologues. Measurements of stable
water isotopes use the ratio of the heavy to light isotopologue for each atom ($R = ^{18}O / ^{16}O$ or $^2H / ^1H$ and are
expressed in delta notation ($\delta^{18}O$ and δ^2H), where $\delta = 1000 * (\frac{R_{sample} - R_{standard}}{R_{standard}})$). Samples with higher ratios may
95 be described as ‘enriched’ with respect to an isotope relative to a reference, whereas those with lower ratios may be
described as ‘depleted’ with respect to an isotope and relative to a reference.

The utility of any tracer comes from ~~their~~ its spatial and temporal variability. In the case of water isotopes as trac-
ers, ~~these arise from~~ variability arises from isotopic fractionation, a physically-governed ‘sorting’ of heavy-atom
bearing water molecules (~~$^1H^2H^{16}O$ and $^1H_2^{18}O$~~ and $^1H^2H^{16}O$) from those bearing only light atoms ($^1H_2^{16}O$) that oc-
100 curs during phase changes (~~i.e., evaporation, condensation, sublimation, deposition~~) ? (i.e., evaporation, condensation, sublimation)
. Spatial and temporal patterns of $\delta^{18}O$ and δ^2H are very similar, as evidenced by the strong correlations between
 $\delta^{18}O$ and δ^2H in precipitation ?? and in other waters, including those in the ground, surface, and soil ??.

Linear relationships between $\delta^{18}O$ and δ^2H in precipitation, and waters derived from precipitation (e.g., ground,
river, lake, soil) are the basis for the ubiquitous water line (WL) framework, in which the best fit lines of the form
105 $\delta^2H = \beta\delta^{18}O + I$ are calculated for different water types (e.g., meteoric (MWL), ground (GWL), surface (SWL))
and are defined either for specific points (local, e.g., LMWL) or for regional or global datasets (e.g., GMWL)
comprising multiple points. Slopes and intercepts of these lines have useful physical interpretations ?, particularly
as they relate to the global average conditions. Global average conditions are represented by the Global Meteoric
Water Line (GMWL), which has a slope of 8 and intercept of 10. Differences between $\delta^{18}O$ and δ^2H , relative
110 to an expected, global average relationship are calculated using a secondary parameter called deuterium excess
(defined as $d = \delta^2H - 8 * \delta^{18}O$). Deuterium excess (d) is used to detect evaporation of precipitation and surface
waters, evaporation under a vapor pressure gradient or non-equilibrium condensation processes, like snow formation
in mixed phase clouds or isotopic fractionation during the melting of snow ~~??????~~.

Because hydrologic processes including groundwater recharge, discharge, and precipitation runoff do not cause
115 isotopic fractionation, we can use water fluxes from hydrologic models with estimates of the isotope ratios of those
fluxes on the appropriate timescales to produce river water isotope estimates. This works well because the groundwa-
ter and runoff fluxes to summertime streamflow in the Western US have distinct stable isotope ratios due to seasonal
and spatial controls on precipitation isotope ratios. The signatures of groundwater inflow and snowmelt tend to have
the lowest isotope ratios of the water sources in the hydrologic system and tend to be relatively temporally invariant
120 ~~?????~~. In contrast, summer precipitation, which contributes runoff to streams, tends to have higher isotope ratios
than groundwater ??.

Anthropogenic modifiers of streamflow that are not included explicitly in the NWM (i.e., irrigation and reservoirs)
may be expected to alter the isotopic signature of streamflow downstream of the ~~river water source areas in the~~

headwaters. Agricultural irrigation can contribute both runoff to streams and recharge groundwater ???. Evapora-
125 tion occurring during conveyance and application increases the isotope ratios in water recharged by irrigation and
decreases d ???. This isotopic signature is passed along to the plants ?. Thus, irrigation-sourced recharge (runoff or
ground) exhibits an evaporated isotopic signature that is distinct from naturally recharged groundwater or precipita-
tion runoff. The effects of evaporation on the isotope ratios of the return flows are expected to be greater in arid areas
with higher summer temperatures and higher vapor pressure deficits. Although lakes can be isotopically enriched
130 with lower d (isotopically evapoconcentrated) relative to other surface waters ?, we do not expect similar signals of
evaporation-driven isotopic enrichment from reservoirs. Relative to natural lakes across the US, evaporation rates
from western lakes are low relative to inflow ?. Instead, reservoirs may alter the isotope ratios of streamflow through
retention of and later discharge of spring snowmelt. Thus, reservoir outflow may have lower isotope ratios and higher
 d than the upstream rivers during the summer months.

135 In this study, we compared hydrologic model-informed estimates of long term mean streamflow isotope ratios
with stream water isotope observations across the western US. The model-informed estimate of river water isotope
ratios used an isotope mass balance methodology that combined the long term average water fluxes of the NWM
and water stable isotope datasets. If the NWM constrains all water sources affecting streamflow, we expect the
differences between the isotope mass balance results and isotopic observations (observation-model differences) will
140 be small and be uniformly positive or negative throughout each basin. If we observe spatial and/or seasonal variability
and structured patterns in observation-model differences within basins (i.e., patterns with elevation, stream order,
or aridity), particularly with respect to the sign of the difference, we may infer that the NWM is incorrectly
partitioning runoff and groundwater fluxes, or missing important water sources. We hypothesize that if we observe
spatial variability and structured patterns in our observation-model difference data, we will observe higher isotope
145 ratios and lower d in more arid reaches reflecting the influence of irrigation return flows, which we expect bear an
isotopic signal of evaporation, on streamflow as compared to higher elevation, humid or seasonally snowy reaches
with minimal anthropogenic influence.

2 Methods

This study analyzes spatial patterns in observation-model differences to evaluate missing sources of streamflow
150 in the NWM in the western US. The ‘model’ estimates are produced using an isotope mass balance approach,
where water fluxes were supplied by NWM simulations of groundwater and surface runoff fluxes ? and isotope
ratios came from gridded groundwater and precipitation stable isotope products (??, Figure 1, Section 2.3). These
mass balance estimates were compared to a large collection of stable river water isotope observations, and both
the compiled observations and mass balance estimates are publicly available (?, Figure 1, Section 2.4). Differences
155 between observations and modeled data were compared in an error-partitioning framework (Section 2.5), and we
tested the hypothesis that spatial variability in observation-model differences contains a signature of agricultural

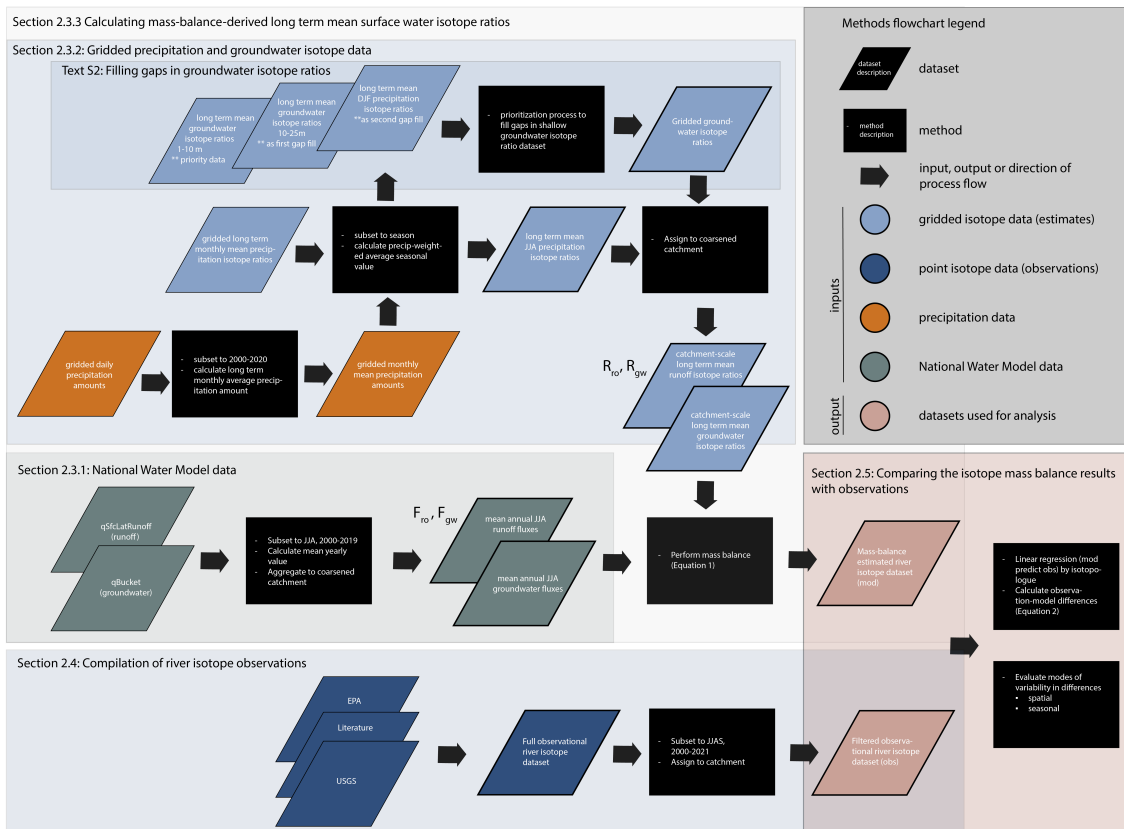


Figure 1. Diagram showing methods and datasets as described in Sections 2.4-2.6. Four datastreams were used to formulate the long isotope mass balance estimates of river isotope ratios: gridded precipitation isotope estimates \hat{R}_{ro} , gridded groundwater isotope estimates \hat{R}_{gw} , gridded precipitation data P and NWM data F_{ro}, F_{gw} . Three data categories contributed to the observational river isotope dataset: USGS R_{ro}^{obs} , EPA R_{ro}^{obs} , and literature datasets accessed from the Water Isotopes database R_{ro}^{obs} .

water use (Section 2.6). A groundwater isotope ratio dataset and a well water surface elevation relative to river surface elevation dataset from R_{gw} were used as independent lines of evidence supporting our analysis of observation-mass balance estimate differences (Section 2.7).

160 2.1 Temporal domain

Our analysis was constrained to summer months (June, July, August) between 2000 and 2019. The specific months chosen reflect those with greatest evapotranspiration and thus consumptive water use and correspond to the season with the largest number of spatially distributed river water isotope observations.

2.2 Spatial domain

165 We selected 5 hydrologic unit 2-digit code (HUC2) scale basins ? in the Western US to compose our study area: the
Upper Colorado (14), Lower Colorado (15), Great Basin (16), Pacific Northwest (17), and California (18). All basins
were characterized by rivers sustained by wintertime snowpack mediated by groundwater infiltration and discharge.
All basins also included water management through impoundments and substantial water use for agriculture. In a
170 arid, whereas much of the northern and mountainous portions of the study area was classified as warm temperate
or seasonally snowy.

The spatial domain and streamflow routing were represented by a network of flowlines (reaches) and catchments
(n=15787, 1:1 flowlines:catchments) derived from the National Hydrography Dataset Plus (NHDPlus, ?, see Text
S1 for network processing details) and clipped to the spatial domain of our study. Catchments had a median size of
175 51 km² and a mean size of 221 km², and flowlines had a median length of 20 km² and a mean length of 32 km². All
data used in this analysis were spatially joined to this network, and we retained attributes provided by NHDPlus
for analysis, including catchment area, Strahler stream order, reach length, minimum and maximum catchment
elevation, and feature code, which denoted the flowline path type.

2.3 Using isotope mass balance to estimate long term mean river isotope ratios

180 Using estimates of long term mean groundwater and precipitation isotope ratios ??, we applied an isotope mass-
balance to the NWM groundwater and surface runoff fluxes to streams (Figure 1). The operational hydrologic
model is based on the open-source, community hydrologic model WRF-Hydro ?? and simulates and forecasts major
water components (e.g., evapotranspiration, snow, soil moisture, groundwater, surface inundation, reservoirs, and
streamflow) in real time across the CONUS, Hawaii, Puerto Rico, and the US Virgin Islands. In the NWM framework,
185 surface and soil evaporation are wrapped into the evapotranspiration flux variable, and direct evaporation from rivers
and reservoirs are not considered in the NWM surface water balance. Thus, we did not apply any additional isotopic
fractionation to the groundwater and surface runoff isotopic fluxes. This approach produced an estimated long term
mean isotope ratio for river reaches in the western US. These estimates were directly comparable to river water
isotope observations.

190 2.3.1 National Water Model data

We accessed lateral surface runoff (NWM variable qSfcLatRunoff, m³ s⁻¹) and groundwater (qBucket, m³ s⁻¹)
fluxes from the NWM v 2.1 Analysis Assimilation dataset ? for our mass balance estimates (Figure 1). The NWM
runoff term (qSfcLatRunoff) only includes surface runoff and does not include subsurface runoff. Instead, subsurface
runoff is routed from the bottom of the soil layer to the groundwater bucket (qBtmVertRunoff). We also accessed
195 streamflow (streamflow, m³ s⁻¹) fluxes as a reach scale quantity to be included in the ~~results analyses~~ analyses

[of results](#). All NWM variables we used are available at the NHDPlus reach scale on an hourly timestep between 2000 and 2019. We subset these variables to the summer months (June, July, and August) and calculated the mean water fluxes to each reach for the summer season of each year. The interannual variability in the summer fluxes was leveraged as an estimate of the uncertainty of the long term mean summer water fluxes.

200 2.3.2 Gridded precipitation and groundwater isotope data

The precipitation and groundwater stable isotope ratios ($\delta^2\text{H}$, $\delta^{18}\text{O}$) that we used to perform the isotope mass balance came from two publicly available gridded products. Both represent long term means or climatologies and provide estimates of uncertainty.

We obtained monthly precipitation isotope ratio climatological predictions and uncertainty estimates (1 standard
205 deviation) for both H and O from ?. The monthly USA grids were available at 1 km, and were produced with the OIPC v3.2 database ? following methods described in ?. Monthly grids have been adjusted for consistency with annual values (~~(see version notes for OIPC2.0 ?)~~ [\(see version notes for OIPC2.0; ?\)](#)). In general, isoscape accuracy depends on the spatial and temporal coverage of point datasets available to produce the isoscape. The ? product is the highest resolution gridded product available for the conterminous United States, and in contrast to other global
210 or regional gridded isotope products, is produced using precipitation isotope ratio data from not only the Global Network of Isotopes in Precipitation (GNIP), but also the US Network of Isotopes in Precipitation, and a host of other precipitation samples collected and stored in the Water Isotopes Database ?. In our input dataset, the median standard deviations of both $\delta^2\text{H}$ and $\delta^{18}\text{O}$ are about 0.12‰, but may be as large as 2-3‰, depending on the region and isotope, based on a N-1 jackknife approach to error estimation ?.

215 We calculated the precipitation-weighted long term mean summer (June, July, August) and winter (December, January, February) seasonal isotope ratio climatologies with long term monthly mean precipitation climatologies calculated from the Climatic Research Unit (CRU) mean monthly precipitation amounts ?? for the period 2000-2020. The precipitation weighted mean seasonal climatology error was calculated analytically from the timeseries.

The groundwater isoscapes used in this analysis were produced by ? for 7 depth intervals ranging from 1 to 1000m.
220 The groundwater isoscapes were not temporally resolved. The authors report errors smaller than 0.71 and 1.07‰ in $\delta^{18}\text{O}$ and $\delta^2\text{H}$ estimates, respectively, based on a cross-validation approach. The approach was validated using an independent dataset and found that variance in the modeled groundwater predicts 92% of the variance in the validation dataset, with no bias. The authors suggest that because the approach estimates groundwater isoscapes at different depth intervals it produces more accurate estimates than methods for producing bulk groundwater
225 isoscapes.

Because this project focuses on groundwater discharge to streams, we preferentially utilized the 1-10m depth interval. However, this layer contained some data gaps where insufficient well data were present to perform an estimate. Where available, we filled these data gaps using either other groundwater depths or mean winter precipitation (DJF)

as described in Text S2. The groundwater isotope ratio data included estimates of uncertainty, which were retained
230 for the characterization of uncertainty around the mass balance isotope ratio estimates.

The gridded precipitation and groundwater isotope datasets and their uncertainties were assimilated to the NHD-Plus spatial framework. Because the raster data grid sizes were larger than the catchment sizes we employed a distance minimization approach using the centroid of the catchment and the centroids of the grid cells.

2.3.3 Calculating mass-balance-derived long term mean surface water isotope ratios

235 To estimate the long term mean surface water isotope ratio ($R_{sw,r}$) at each reach (r) in the spatial domain (Equation 1), we accumulated the groundwater (gw) and surface runoff (ro) isotope fluxes (i.e., the isotope ratio multiplied by the water flux, $R * F$) for all reaches (i) from the headwaters downstream to the reach. The isotope ratio for surface runoff (R_{ro}) came from the summer mean gridded precipitation isotope ratios and the isotope ratio for the groundwater flux (R_{gw}) came from the gridded groundwater isotope ratios (see Section 2.3.2). The summed isotope
240 fluxes were divided by the summed surface runoff and groundwater fluxes.

$$R_{sw,r} = \frac{\sum_{i=0}^r R_{gw,i} * F_{gw,i} + R_{ro,i} * F_{ro,i}}{\sum_{i=0}^r F_{gw,i} + F_{ro,i}} \quad (1)$$

Our long term mean estimates of $R_{sw,r}$ are subject to uncertainty from 1) internannual variations in the mean summer volumetric contributions of groundwater and surface runoff to streamflow and 2) because the long term mean estimates of the groundwater and precipitation isotope ratios are subject to uncertainty arising from underlying data
245 coverage as well as interannual variability. To constrain uncertainty in our long term mean estimates of $R_{sw,r}$, we calculated 200 estimates of R_{sw} per reach by taking 10 random draws of from the isotope ratio distributions (assuming a normal distribution), for each of the 20 years of record. This approach uses interannual variability in surface runoff and groundwater fluxes to constrain the variability in the water flux component of the calculation, and uncertainty in the isotope ratio estimates to constrain the uncertainty in the isotope ratio component of the calculation. Joint
250 distributions (of either H and O, or isotopes with water fluxes), were not used because information about how the isotope ratios might covary was not available from the gridded isotope datasets and no assumptions were made about how the isotopes might vary with interannual variability in climatic conditions. Similarly, no assumptions were made that the precipitation and groundwater isotope ratios covaried in time. These 200 estimates were used to calculate a long-term mean estimated isotope ratio for river water in each reach of the network and to evaluate uncertainty
255 in our estimates.

2.4 Compilation of river isotope observations

The results of the mass balance [calculations](#) were compared with observations of stable water isotope ratios from rivers collected between 2000 and 2021, during the growing season months of June, July, August and September. We included two additional years (2020 and 2021) as well as data from the month of September beyond the temporal
260 constrains of the NWM model domain in our set of observations. This decision was made to maximize the amount

of data and number of unique river reaches in the spatial domain that are available for analysis, and reflects the assumption that the long term mean river isotope ratios calculated from the mass balance approach will be insensitive to inclusion or exclusion of a small number of additional years or an additional growing season month.

We compiled surface water stable isotope ($\delta^2\text{H}$, $\delta^{18}\text{O}$) measurements from various sources including the Environmental Protection Agency (EPA), the United States Geological Survey (USGS) National Water Information System (NWIS, ?), and published datasets assimilated in the Water Isotopes Database ?. Not all reaches had one or more stable water isotope observations, and river reaches with multiple stable water isotope ratio observations were sometimes, but not always, from the same sampling site within the catchment.

The EPA surface water stable isotope data came from the National Rivers and Streams Assessments (NRSA, ??) and the National Lakes Assessment (NLA, ??). These data were collected once or twice per summer on a five year rotating basis as part of routine sampling campaigns. Over the time period of our analysis, we obtained three collections of NRSA samples (2008-2009, 2013-2014, and 2018-2019). Sites were sometimes but not always resampled among the campaigns. Sampling was stratified based on Strahler stream order and by state ensuring that all orders were sampled within each state in the assessments ?. This means that higher order reaches are less frequently sampled than medium or low order reaches.

The USGS surface water stable isotope data for rivers were downloaded through the NWIS API ? and the literature data came from published and unpublished sources that are publicly available through the Water Isotopes Database ?. Stable isotope collections are not part of routine measurements for the USGS, but rather are collected by specific USGS projects. Thus, stable isotope data collections from the USGS and literature datasets tended to be spatially and temporally clustered.

2.5 Comparing the isotope mass balance results with observations

The relationship of the NWM isotope mass balance (modeled) to the river isotope observations were evaluated using correlation and simple regression analyses, where the modeled isotope ratio (either $\delta^2\text{H}$ or $\delta^{18}\text{O}$) values are used to predict the observed isotope ratios. We evaluated the results with all unaveraged observations and mean isotope ratio at river reaches with multiple observations. A Pearson correlation analysis was performed using the 'corr()' function of python's 'pandas' package ?. Regression analysis was performed using the ordinary least squares (OLS) function in the python 'statsmodels' package ?.

We calculated the likelihood that an observation and the model result came from the same distribution, based on the variance in the model estimate, and variance associated with river water isotope observations (Text S3) using a two-tailed t-test. We reported p-values, where $p < 0.1$ indicated that the isotope mass balance estimate was statistically different from the observed surface water isotope ratio for the specific element (H or O).

2.5.1 Calculating observation-model differences

We calculated the observation (*obs*)-model estimate (*mod*) differences in both $\delta^{18}O$ and δ^2H , by subtracting the model estimate from the observation ($\delta^{18}O_{diff} = \delta^{18}O_{obs} - \delta^{18}O_{mod}$; $\delta^2H_{diff} = \delta^2H_{obs} - \delta^2H_{mod}$). Using both isotope systems, we established a framework for interpretation of our results (Figure 2) that utilizes movement along or deviation from the global mean $\delta^2H : \delta^{18}O$ ratio of 8 that is used to represent fractionation that occurs at equilibrium and defines the slope of the Global Meteoric Water Line (GMWL, ~~?~~)(GMWL, ~~?~~).

Observation-model differences may arise from either 1) incorrect model source representation (i.e., missing water sources or incorrect fluxes of established sources) or 2) errors in the isotope ratio datasets used for the isotope mass balance calculation. Thus, for positive or negative values of $\delta^{18}O_{diff}$ and δ^2H_{diff} that exhibit a $\delta^2H_{diff} : \delta^{18}O_{diff}$ ratio of 8, we infer either errors in NWM with respect to the proportions of surface runoff and groundwater contributed, or errors in the gridded isotope ratios (likely groundwater, due to its disproportionate contributions to streamflow). For positive or negative $\delta^{18}O_{diff}$ and δ^2H_{diff} with $\delta^2H_{diff} : \delta^{18}O_{diff}$ ratios different from 8, we infer that the NWM is missing uncharacterized water sources with isotope values bearing a signature of non-equilibrium fractionation. We quantify differences of $\delta^2H_{diff} : \delta^{18}O_{diff}$ ratios from 8 using a metric of similar to d (Equation 2).

$$d_{diff} = \delta^2H_{diff} - 8 * \delta^{18}O_{diff} \quad (2)$$

We can interpret combinations of $\delta^{18}O_{diff}$ and d_{diff} together, as well as d_{diff} independently to infer the uncharacterized sources responsible for the observation-model difference. This framework is useful because the ratios of δ^2H to $\delta^{18}O$ of the isotopic inputs to the isotope mass balance tend to be close to 8 ?? whereas those from the observations more often differ from 8 ??. This means that all non-zero d_{diff} values can be used to identify omitted water sources with non-equilibrium fractionation signals and can be used to diagnose where these sources may contribute to streamflow. The conditions of this study, based on the data and approach, mean that the mass balance approach represents a null hypothesis that all processes and sources contributing to streamflow carry an isotopic signal of equilibrium fractionation (i.e., precipitation, groundwater, routing). In other instances, where the modeled approach could reflect a combination of equilibrium and non-equilibrium processes, the interpretation of observation-model differences, particularly in terms of the d_{diff} axis, may change.

2.6 Evaluating variability in observation-model differences

Following the spatial strength of our dataset, which relies heavily on the EPA NRSA datasets, we focused on evaluation of spatial variability in observation-model differences in our dataset. We evaluated temporal variability to 1) support findings from our analysis of spatial variability and 2) determine whether there may be spatial-temporal covariance which influences our results.

Spatial structure in the observation-model differences were evaluated graphically by comparison of $\delta^{18}O_{diff}$ and d_{diff} with catchment mean elevation, Strahler stream order, and Köppen climate class ?. The former two variables

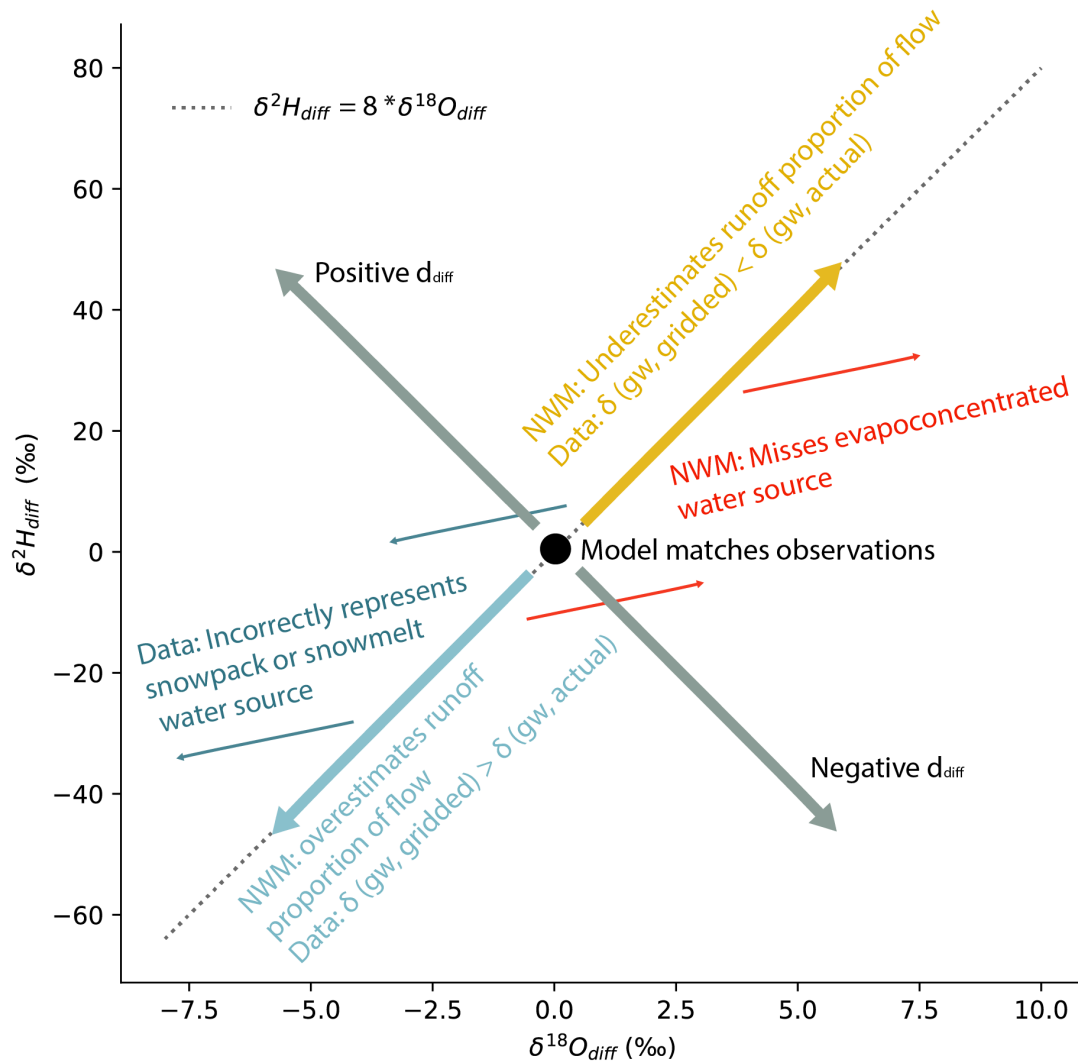


Figure 2. Schematic for interpretations of observation model differences utilizing dual isotope difference space and assumptions about the expected relationships between $\delta^{18}O_{diff}$ and δ^2H_{diff} . The annotations associated with ‘NWM’ specify the sort of hydrologic model error (i.e. water source apportionment) that could produce the observation-model comparison result, if all isotope data supplied to the isotope mass balance are correct. The annotations associated with ‘Data’ specify the sort of error in the gridded isotope datasets that could produce the observation-model result if all NWM water source contributions are assumed to be correct. The interpretations of the secondary mode of variability, captured by d_{diff} , depend on the ‘model’ producing results that reflect equilibrium relationships between $\delta^{18}O$ and δ^2H .

were retained from the NHDPlus catchment dataset ?. The former was joined to the spatial framework as described
325 in Text S4.

Spatial structure in the observation-model differences were evaluated statistically with linear mixed effects mod-
eling using the basin (HUC2) as a random variable using the python ‘statsmodels’ module and the ‘mixedlm()’
function ?. Linear mixed effects modeling with basin as the random (grouping) variable was selected for the analysis
method because water in streams at low elevations is likely to be more isotopically similar to water in the basin
330 headwaters than a nearby stream in a different basin with different water source regions. Thus, we assume the
groups are likely to have different mean values reflecting their hydrologic and climatic differences. Although we also
expect that the relationship of the response variable d_{diff} to the explanatory variables may differ among basins,
both our response and explanatory variables contain substantial scatter as well as small numbers of high leverage
points in each basin, such that a more nuanced analysis that includes temporal aspects of variability would be likely
335 to produce misleading results.

Using the linear mixed effects approach, we tested the statistical relationship between d_{diff} and the ratio of
actual evaporation to precipitation ($\frac{ET_a}{P}$, Text S4), catchment mean elevation, fraction of streamflow estimated to
come from agricultural return flows (Text S5), and a categorical variable indicating influence of large reservoirs
(capacity >50,000 acre-feet, Text S5.2). We performed statistical analysis on all ~~sites on~~ streams not categorized as
340 intermittent, ditches, or canals.

To assess how the observation-model difference may change over the growing season, in which the relative fraction
of agricultural water in a waterway may increase due to low flows and increased water use, we obtained all sites-year
combinations where there were at least three observations during at least three of the four months (Jun-Sep) of the
growing season. We required one of the months be the month of June. From the June value(s) of $\delta^{18}O_{diff}$ and d_{diff}
345 for a site-year combination, we subtracted the $\delta^{18}O_{diff}$ and d_{diff} values calculated for other months at the same
site and from the same year. We evaluated the distribution of the aggregate results, as well as the distributions at
the HUC2 basin scale by comparing their means and interquartile ranges.

Interannual variability was also assessed (Text S6) to ensure that patterns in the other modes of variability did
not arise due to either covariability in spatial and temporal patterns of sampling, or the timescale difference between
350 our isotope mass balance estimates (long term mean) and observations (instantaneous).

2.7 Evaluation of independent lines of evidence supporting signature of agricultural water use in rivers

Because it is difficult to disentangle the effects of elevation and aridity from the effects of human water use and
management due to their spatial covariance, we utilized analyses of independent datasets to support the results of
355 our statistical inference. The analyses evaluated relationships between land use or cover and groundwater isotope
ratios and the fraction of well water levels that are below the nearby river level in catchments across the western
US.

2.7.1 Associating groundwater stable isotope observations with land use / land cover types

Estimates of the isotopic evapoconcentration of groundwater associated with different land use and land cover classes supports our inferences from observation-model differences. We made the associations between groundwater isotope ratios and land use classes at a HUC12 scale ?.

We considered five land use type categories that were aggregations of two or more National Land Cover Database ? categories. The ‘desert’ category was composed of barren land (NLCD code=31), shrub/scrub (52), and grassland-/herbaceous (71) land classes. The ‘forest’ category was composed of evergreen, deciduous and mixed forests (41-43). The ‘developed’ category was composed of all the ‘developed’ classes, including open (21-24). The ‘agriculture’ category was composed of pasture/hay (81) and cultivated crops (82). The final category, ‘water and wetlands’ included all other land types, which include open water (11), perennial ice/snow (12), woody wetlands (90) and emergent herbaceous wetlands (95). We assigned the dominant land use/land cover category for each HUC12 using data based on the land use type with the greatest fractional coverage.

We compiled groundwater stable isotope ($\delta^{18}O$, δ^2H) measurements from the USGS NWIS ?, and published datasets assimilated in the Water Isotopes Database ?. The groundwater isotope ratio observations were spatially joined to the hydrologic units. We did not place temporal or well depth constraints on the samples used in our analysis. Not imposing well depth constraints may contribute to scatter associated with differences in water sources recharging shallow groundwater compared to deeper confined aquifers.

2.7.2 Evaluation of NWM groundwater discharge with well level fractions

The ? dataset compared river surface elevations with river-side well water elevations within catchments. The approach produced the fraction of wells in a catchment whose water surface levels were lower than the water surface level of the nearby river. In catchments where most well water levels are below the river water level (scores close to 1), we expect the river to lose water to shallow groundwater recharge under the right geologic conditions (e.g., permeability). In contrast, in catchments where most well water levels are above the river water level (scores close to 0), we expect groundwater discharge to streams.

We predicted the long term mean summer NWM ‘qBucket’ magnitude using the ? dataset using a simple linear regression. This approach tests the hypothesis that if NWM accurately represents groundwater discharge to streams, the relationship of well water elevations to river surface elevation would predict the summer mean NWM groundwater discharge flux (assuming a linear relationship between the two quantities), with some scatter to account for subsurface permeability and spatial variability in groundwater discharge rates. We then evaluated the effect of agricultural irrigation in a catchment on the relationship between NWM ‘qBucket’ (binned by to the 0-20th, 20th-40th, 40th-60th, 60th-80th, and 80th-100th percentiles) and the ? dataset. The evaluation was split into reaches influenced by irrigation sourced from groundwater and irrigation sourced from surface water, as well as reaches uninfluenced

390 by irrigation water. Irrigation contributions and irrigation water sources were determined using the methods for
estimating irrigation water use described in Text S5.1 and used elsewhere in our analysis.

3 Results and discussion

3.1 Evaluation of the isotope mass balance approach for estimating surface water isotope ratios

Our analysis evaluated 4503 stream stable isotope observations in 877 unique river reaches across the western
395 United States relative to NWM-driven isotope mass-balance-derived estimates (hereafter, ‘modeled’) of the river
isotope ratios. Of these, 448 reaches had more than one observation (often all at the same sampling site in the
catchment, but sometimes at multiple sites, Figure S1), and up to 571 observations in a catchment (Figure S1 and
S2). On average, across all data, the observations were significantly greater than the modeled values by $0.537 \pm$
 0.033 ‰ and 4.81 ± 0.222 ‰ for $\delta^{18}O$ and δ^2H , respectively (Figure 3). For $\delta^{18}O$ we observed a standard deviation
400 of 3.16‰ for the observed data and 2.96‰ for the modeled data (for all data averaged by catchment). For δ^2H we
observed a sample standard deviation of 25.4‰ for the observed data and 24.4‰ for the modeled data (for all data
averaged by catchment, Figure 3).

We calculated surface water lines (SWL) for both the modeled and observed results using all available data
(Figure 3). The observations yielded a SWL with a slope of 7.570 (± 0.023), and intercept of 1.2301 (± 0.320),
405 which was significantly different from the slope of the GMWL slope of 8 and intercept of 10 and was within the
range of local MWLs (LMWL) slopes for western North America (6.5-8) †, reported in Table 1. The model results
yielded a surface water line with a slope of 8.12 (± 0.010) and an intercept of 8.06 (± 0.14) which was more similar
to, but still statistically different from the GMWL and differed from LMWLs for the region (Table 1). Comparison
of the observation and modeled data distributions and water lines reveals evidence for evaporation of surface waters
410 in the observations but not in the isotope mass balance results (Figure 3). This is because the primary source of
streamflow in the modeling framework, high elevation groundwater discharge, does not bear an evapoconcentrated
isotopic signature in our input ~~datasets~~dataset, and lower elevation water sources (groundwater or surface runoff)
that could bear an isotopic signature of evaporation, depending on the region, are considered by the model to be
minor contributors to streamflow over the timescale integrated by our study.

415 Despite the differences in the data distributions, the modeled isotope ratios and observed isotope ratios were
well correlated (Table 2, Figures S4-7), with correlation coefficients between 0.761 and 0.866, depending on the iso-
topologue and whether individual observations or catchment means were considered. These correlations translated
to statistically significant simple linear regressions where the modeled isotope ratios were used to explain the ob-
served isotope ratios (Table 2). Depending on the isotopologue and whether individual observations or means were
420 considered, the ~~model~~models explained between $\sim 58\%$ and 75% of the variance in the observations. The model
explained more variance for δ^2H than $\delta^{18}O$, and more variance for catchment mean values relative to individual
observations. For all regressions, the slopes ranged from 0.879 to 0.937, with catchment mean slopes tending to be

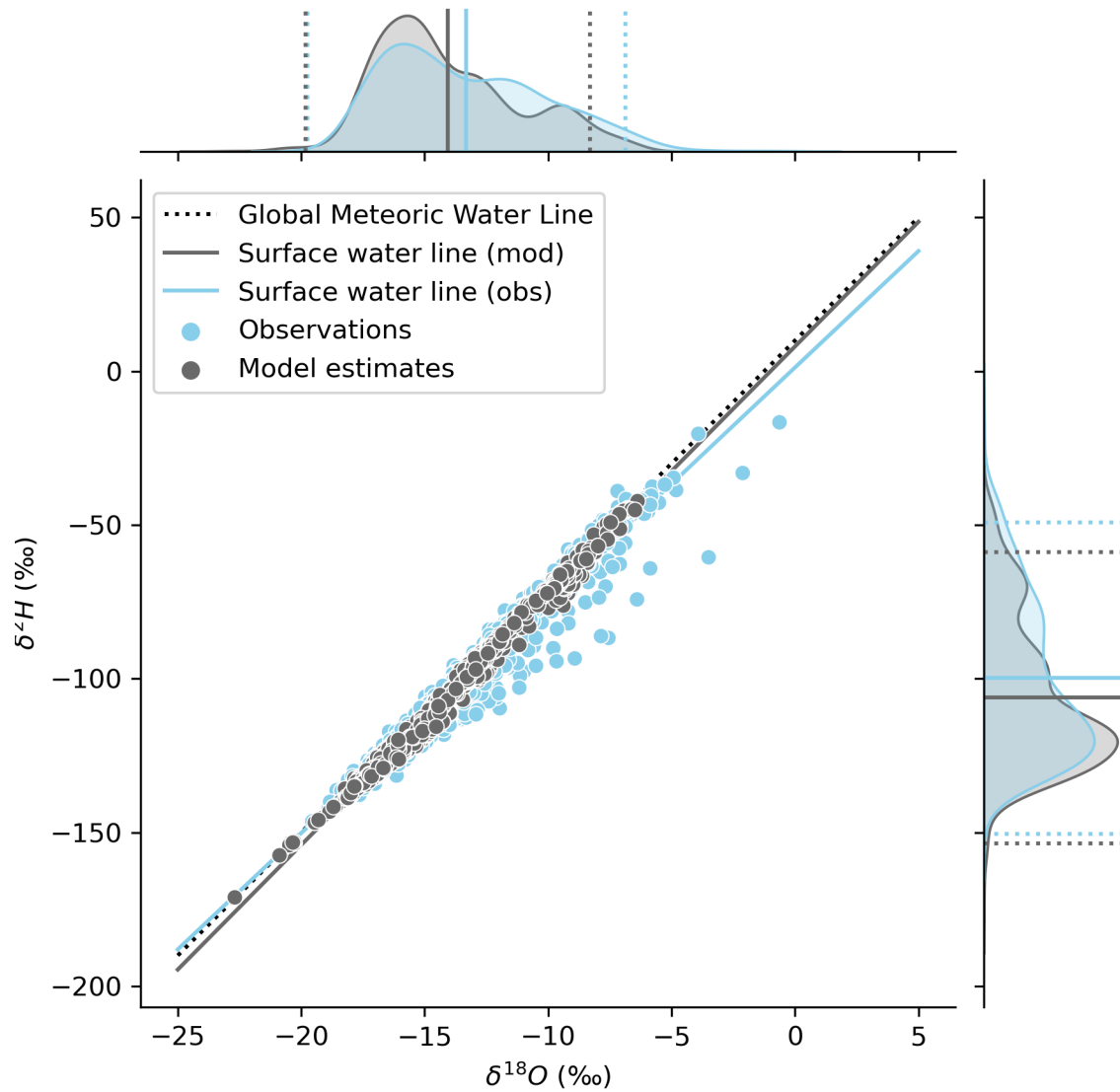


Figure 3. The distribution of the catchment mean observation (obs, blue) and isotope mass balance estimates (mod, gray) ($n=448$) with the Global Meteoric Water line (dotted) and the two datasets' surface water lines (solid lines). See Table 1 for water line statistics. Data distributions, including mean and two standard deviations of each data type (dotted lines), are shown in the plot margins. Observations plotting below the GMWL indicate evaporation, while those plotting above the GMWL may indicate mixed phase cloud processes or other non-equilibrium condensation processes ?.

Surface water lines:	β (\pm s.e.)	I (\pm s.e.)	R ²
Model-derived	8.12 (\pm 0.010)	8.06 (\pm 0.14)	99.3%
Observations	7.57 (\pm 0.02)	1.23 (\pm 0.32)	96.1%
Meteoric water lines:	β_{min}, β_{max} (β_{avg})	I_{min}, I_{max} (I_{avg})	
Global Meteoric Water Line	8	10	
Arid and Temperate dry summer LMWLs	6.56, 8.02 (7.57)	-10.5, 9.85 (3.02)	
Temperate humid and Continental LMWLs	7.34, 7.64 (7.49)	-3.82, 3.31 (0.62)	

Table 1. Surface water line slopes and intercepts ($\delta^2H = \delta^{18}O + I$) compared to the Global Meteoric Water Line and published precipitation water line ranges (LMWLs) from different climate classifications in North America (data from ?). Because all regressions are highly significant, no p-values are shown.

Statistical model	n	Corr. coef	β (\pm s.e.)	I (\pm s.e.)	R ²
$\delta^{18}O_{obs} \sim \delta^{18}O_{mod} + I$	4503	0.761	0.917 (\pm 0.012)*	-0.645 (\pm 0.168)*	57.9%
$\delta^{18}O_{obs,avg} \sim \delta^{18}O_{mod,avg} + I$	448	0.820	0.879 (\pm 0.029)*	-0.891 (\pm 0.414)*	67.3%
$\delta^2H_{obs} \sim \delta^2H_{mod} + I$	4503	0.819	0.937 (\pm 0.010)*	-1.90 (\pm 1.06)*	67.1%
$\delta^2H_{obs,avg} \sim \delta^2H_{mod,avg} + I$	448	0.866	0.905 (\pm 0.025)*	-3.10 (\pm 2.66)	75.1%
$\delta^2H_{diff} \sim \delta^{18}O_{diff} + I$	4503	0.959	6.54 (\pm 0.029)*	1.30 (\pm 0.065)*	91.9%
$\delta^2H_{avg,diff} \sim \delta^{18}O_{avg,diff} + I$	448	0.958	6.70 (\pm 0.094)*	1.46 (\pm 0.190)*	91.9%

Table 2. Correlation and regression results for observation-model comparisons. Regressions were performed on all data (n = 4503), as well as on the mean values in a subset of the reaches with more than one observation (n=448). An asterisk (*) indicates the coefficient is significant at p<0.1.

lower than slopes calculated from all observations. Intercepts for all regressions were close to, but less than 0, with lower intercepts associated with regressions calculated from catchment mean values, relative to regressions calculated from all observations. The statistically significant slopes of less than 1 and statistically significant intercepts arise in all observation-model comparison regressions because the observations tended to exhibit higher isotope ratios than the model estimated at the lower end of the isotopic distribution (Figures S4-7). Many of the catchments characterized by this pattern were in ~~more arid locations~~ arid regions. The greater variance explained by the regressions using catchment means relative to the individual observations suggest that using a time varying inputs rather than calculating a long term mean river isotope ratio may further improve observation-model comparisons.

3.2 Model-observation differences

Of 4503 observations, 1763 $\delta^{18}O$ and 3306 δ^2H observations were significantly different from the long term mean isotope mass balance NWM estimate at p<0.1. Of these, 1756 observations indicated significant differences for both

$\delta^{18}O$ and δ^2H . This corresponded to a median absolute difference of 2.2‰ for $\delta^{18}O$ and 9.7‰ for δ^2H . For both,
435 a larger proportion of the distribution indicated positive significant differences and those differences tended to be
greater in absolute magnitude than the negative significant differences.

We used an observation-model difference interpretation framework (Figure 2) to gain process information that
can be used to improve our understanding of terrestrial water balance and process inclusion in the NWM. The
observation-model differences in $\delta^{18}O$ and δ^2H were correlated (Figure 4) and yielded similar results for analyses
440 performed with all data as compared to means of reaches with multiple observations (Table 2). Simple linear re-
gressions, where variance in $\delta^{18}O_{diff}$ explained variance in δ^2H_{diff} , with all data and catchment mean data both
explained about 92% of the variance, were significant and exhibited slopes of less than 8 (Table 2), suggesting the
presence of errors arising from NWM omission of water sources that bear signatures of non-equilibrium processes.

In our dataset, model estimates do not deviate much from the GMWL, and deviate less than the observations
445 (Figure 3). The model estimates reflect an assumption that water sources contributing to streamflow were subject
only to equilibrium ~~fraction~~fractionation, whereas observations indicate contributions of waters influenced by non-
equilibrium processes. This information is quantified using d_{diff} (Figure 2). Positive values of $\delta^{18}O_{diff}$ tended to
be associated with negative values of d_{diff} (Figure S8). The shape of the relationship between the two quantities
is non-linear, with a stronger relationship between $\delta^{18}O_{diff}$ and d_{diff} among data from arid reaches compared to
450 humid reaches.

The relationship between $\delta^{18}O_{diff}$ and d_{diff} , as well as our regression (Table 2) and surface water line analyses
(Table 1) indicate that the modeling approach for estimating long term isotope ratios of rivers produce results
that are similar to, but on average, lower and exhibit less variability than observations. The strongest signal in our
data is that of evaporation, evidenced by combinations of positive $\delta^{18}O_{diff}$ and negative d_{diff} in arid regions. We
455 also observe evidence of non-equilibrium condensation processes in reaches characterized by negative $\delta^{18}O_{diff}$ and
positive d_{diff} .

We suggest that patterns in $\delta^{18}O_{diff}$ and d_{diff} contain useful model diagnostic information that can be useful
for improving the NWM and our understanding of the terrestrial water balance. However, the observational dataset
is composed of a non-uniform compilation that contains spatial, seasonal, and interannual modes of variability. Due
460 to the underlying sample collection approaches, the strength of our dataset is evaluating spatial variability, so we
focus our analysis on that mode to gain information about missing water sources that may influence the model.
We support our findings using the temporal evolution of ~~water throughout~~observation-model differences through
the growing season. Based on an analysis of the interannual variability (Text S6) we suggest that the spatial and
temporal structure of our data are sufficiently robust and evenly distributed with respect to interannual variability
465 to support the analysis. Additional sources of variability are discussed in Text S7.

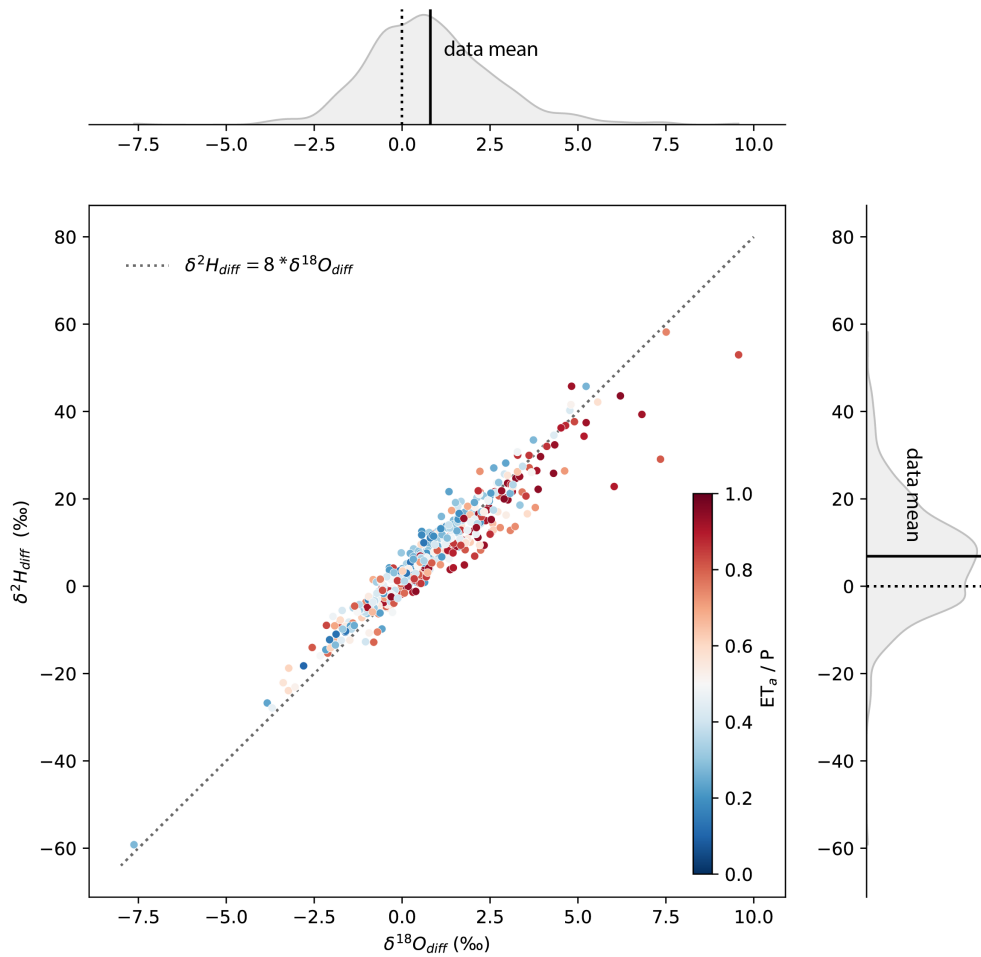


Figure 4. The relationship of observation (obs)– isotope mass balance (mod)–estimation differences for $\delta^{18}O$ and δ^2H . Interpretations of the scatterplot follow the framework indicated in Figure 2. The catchment mean value is plotted, and only sites with at least two observations are shown ($n=448$). The equilibrium line with slope 8 is plotted for context (dotted line), and data are colored by their site’s the ratio of actual evaporation to precipitation. Data distributions are shown for both $\delta^{18}O_{diff}$ and δ^2H_{diff} in the margins, along with the mean differences indicated as a solid line. No difference (0) is marked with a dotted line for reference.

3.3 Spatial distribution of observation - model differences

If the NWM fully constrained all relevant water sources, we expect to observe similar values of $\delta^{18}O_{diff}$ and d_{diff} throughout each basin, irrespective of the location of the observation in the basin. This is because the majority of water discharged to streams in these basins comes from upper elevation water source areas, and [based on the](#)
470 [assumptions of the NWM framework](#), little addition or modification of river waters is expected downstream of headwater catchments. Thus, we expect the observation-model differences calculated in headwater areas would propagate to lower elevation areas in the absence of additions from unconstrained water sources and/or river water modifications from unconstrained processes.

Instead, we observed spatial variability (Figures 5 and S9), where smaller magnitude $\delta^{18}O_{diff}$ values occurred in
475 the highest elevation, lowest stream order, and least arid reaches, and larger magnitude, often positive $\delta^{18}O_{diff}$, values occurred in lower elevation, arid or intermittent flow reaches (Figure S10). d_{diff} tended to exhibit higher values in higher elevation, lower stream order reaches, and lower values in lower elevation, more arid, higher stream order reaches (Figure 6). We observed a greater range in the absolute magnitudes of $\delta^{18}O_{diff}$ and d_{diff} in higher order, lower elevation reaches (Figures 6 and S10). Notably, the pattern was similar across basins, suggesting the
480 importance of within-basin processes in determining $\delta^{18}O_{diff}$ and d_{diff} , as opposed to absolute relationships of $\delta^{18}O_{diff}$ and d_{diff} to elevation, stream order, or climate classification.

The spatial pattern in d_{diff} (Figure 5) was similar to the pattern observed for the KGE and other metric evaluations of the NWM ?. Areas with negative d_{diff} tended to correspond to areas with poor NWM performance ?. However, the isotopic evaluation of NWM and the ? datasets could not be directly compared due to there being
485 only a small number of reaches with both isotope observations and daily discharge measurements.

The spatial structure of our results was statistically well explained by the the ratio of actual evaporation to precipitation ($\frac{ET_a}{P}$) in a linear mixed effects model with basin as the grouping variable (Table 3). Variability among basins explained 16.2% of the variance in d_{diff} , while the fixed effect of aridity explained 13.9% of the variability in the dataset. The regression slope associated with the fixed effects of aridity was negative (-7.87 ± 0.78) and significant
490 ($p < 0.01$), indicating that sites with higher aridity indices tended to exhibit more negative d_{diff} . This regression was stronger than a linear mixed effects model with elevation predicting d_{diff} , where the fixed effects of elevation explained 4.7% of the variability in d_{diff} .

Analysis of the spatial variability in our results suggest that 1) higher elevation, lower stream order, perennial, warm temperate or seasonally snowy reaches had small $\delta^{18}O_{diff}$ and positive d_{diff} values and 2) lower elevation,
495 higher stream order, arid and sometimes intermittent stream reaches had larger and more positive $\delta^{18}O_{diff}$ values and more negative d_{diff} values. The first point suggests errors associated with the challenges of providing input values at appropriate temporal resolutions, [including representing direct snowmelt contributions o streamflow ?](#), whereas the second point suggests the model is missing critical evapoconcentrated water sources in more arid, lower elevation areas of each basin.

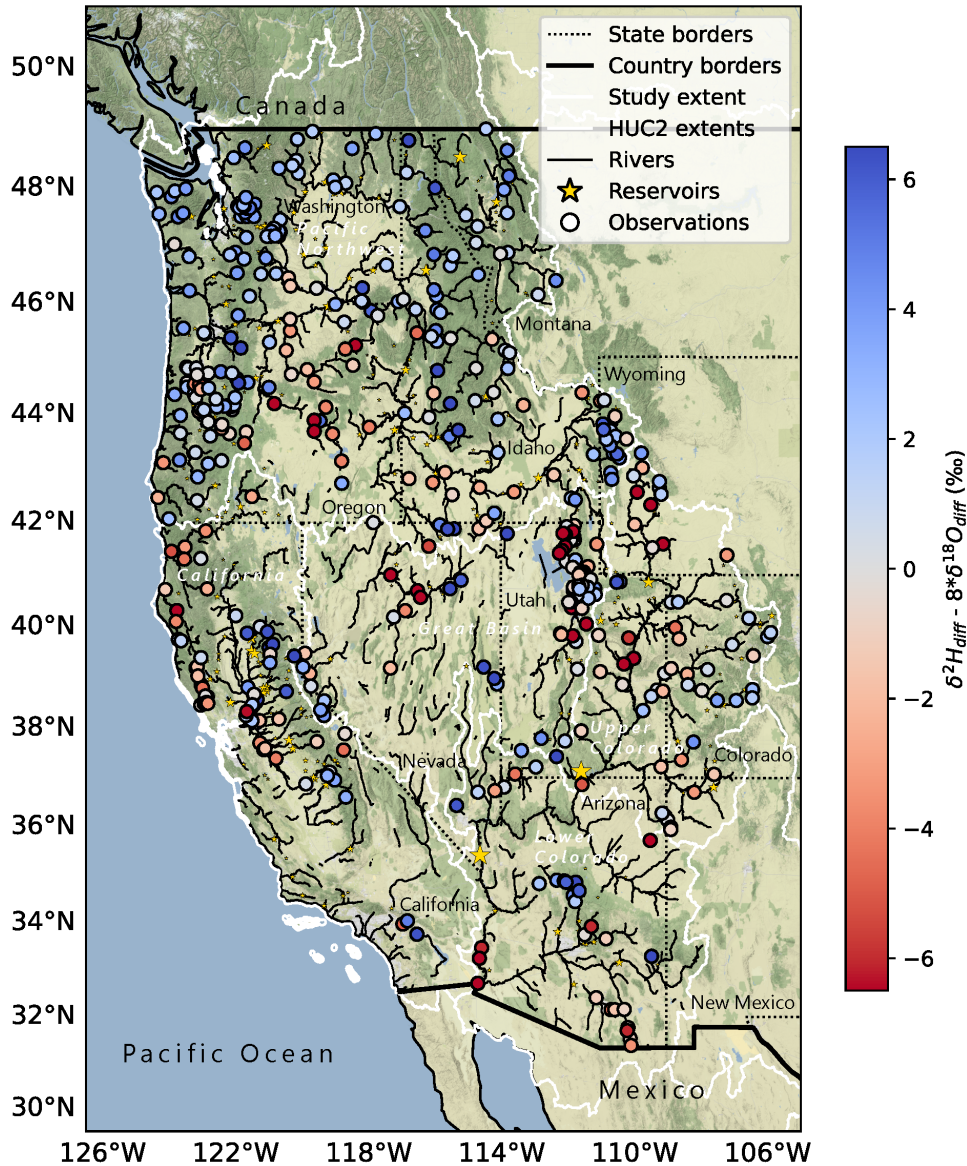


Figure 5. The spatial distribution of mean catchment d_{diff} ($\delta^2 H_{diff} - 8 * \delta^{18} O_{diff}$) in reaches with more than one observation (n=448). Locations of reservoirs Reservoirs are marked by yellow stars, with the star size proportional to the reservoir capacity.

Redder symbols correspond to waters with stronger evaporation signals than expected based on the model estimate. Map

data is from ©OpenStreetMap contributors 2023, distributed under the Open Data Commons Open Database License (ODbL)

v1.0, accessed through Stamen OpenSource Tools (<https://stamen.com/open-source/>). HUC2 basins come from WBD ? and

rivers are modified from the NHDPlus streamline network ?.

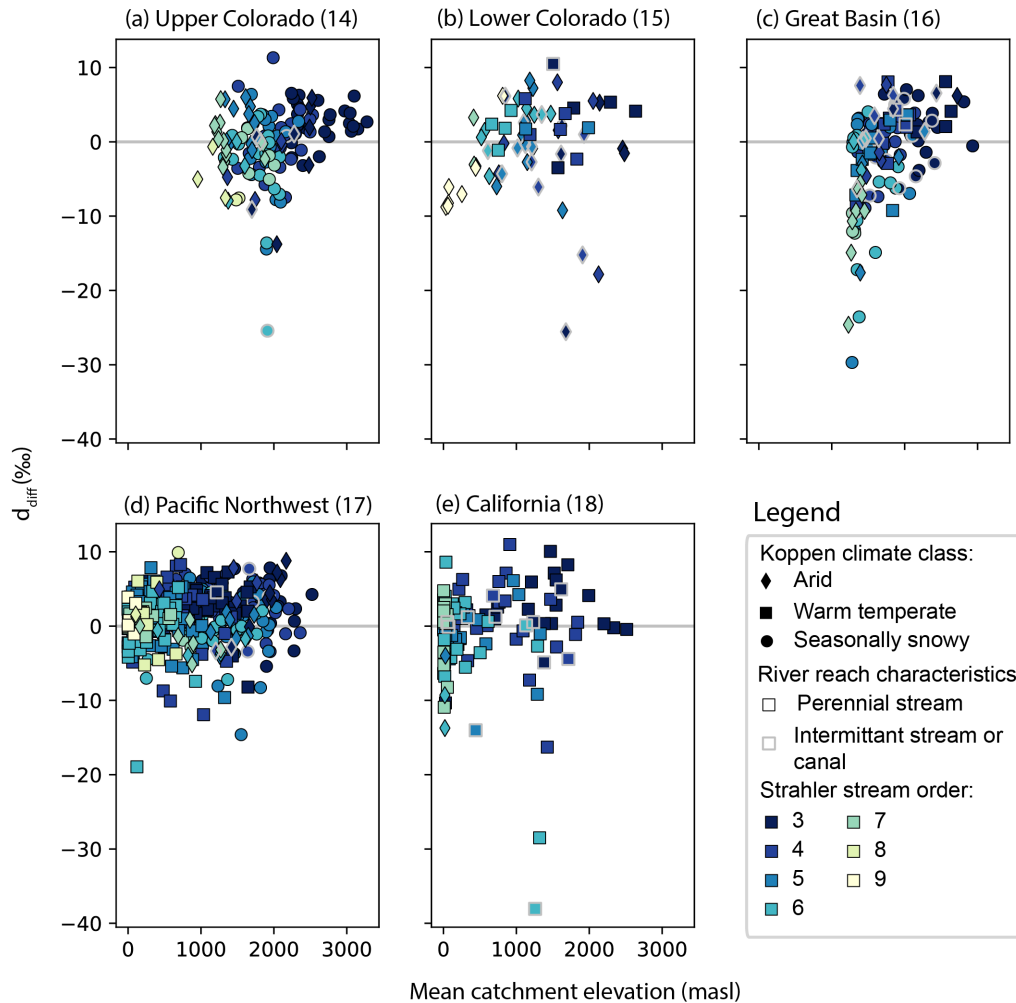


Figure 6. Relationship of elevation, Strahler stream order, and Köppen climate classification, and stream persistence to d_{diff} in each basin. We observe higher d_{diff} in perennial, lower order streams at middle and higher elevations in each basin. Lower d_{diff} is associated with higher order streams at lower elevations in each basin. This effect was greater in catchments classified as arid or seasonally snowy compared to those classified as warm temperate. This pattern was generally true in each basin, irrespective of the absolute elevation or stream order, suggesting the importance of accumulated effects within a basin on d_{diff} .

500 3.3.1 Observation-model differences in headwater reaches reflect groundwater isotope ratio estimates

We observe $\delta^{18}O_{diff}$ and d_{diff} values that are statistically different from 0 in higher elevation, low stream order, low aridity, temperate or seasonally snowy reaches in our dataset (Figures 6, S10). These differences tend to be smaller than than the full dataset mean $\delta^{18}O_{diff}$ and d_{diff} . At most of these reaches we also observe positive d_{diff} values (Figures 5, 6).

The presence of both negative and positive values of $\delta^{18}O_{diff}$ likely reflect interannual variability in the isotope ratios of actual groundwater and snowmelt discharged to rivers in high elevation headwater areas. Although groundwater's contribution to streams is conceptualized in this study to be constant in magnitude and isotope ratio, the isotope ratios of both groundwater and snowmelt fluxes vary spatially and interannually. The groundwater flux magnitudes vary interannually based on variations in snowpack magnitudes, antecedent hydrologic conditions ??, and hydrogeologic ? controls including hydrologic residence times. Snowpack isotope ratios vary in response to climate patterns and local conditions ? and the imprint of snowmelt on river isotope ratios depends on melt timing and contributing elevations ?. The observed variability of $\delta^{18}O_{diff}$ does not exhibit a uniform tendency towards positive or negative values. This suggests the mean groundwater isotope ratios used in this study are reasonably representative of the long term mean estimates of the isotope ratios of water contributed at high elevation water source areas by groundwater and snowmelt fluxes, though improvements may be made by using ~~interannually varying estimates of the isotope ratios of a~~ time-varying approach, where estimates of groundwater and snowmelt isotope ratios vary with month and year. However, the systematic positive d_{diff} result cannot be explained by the timescale of the isotope input.

Higher d streamflow relative to weighted mean precipitation values have been documented in other studies ?. This may be because higher d is associated with lower precipitation $\delta^{18}O$ that falls during the cold season in mid-latitude regions, particularly in areas near open water ????. Secondly, high d in rivers relative to precipitation or groundwater may be attributed to fractionation occurring during melt. The snow melt process has been demonstrated to begin with preferential melt of water molecules bearing lighter isotopologues, and to exhibit higher d earlier in the melt season ????. Further, a recent study suggested this signal may be used to identify the elevation of snowmelt contributing to streamflow during the melt season ?. The higher d of the snow and initial meltwater may be passed along to the rivers via direct surface runoff to streams or through shallow groundwater recharge and rapid discharge to streams (see the relatively higher upper bound on d values for forested land use types in Figure 7).

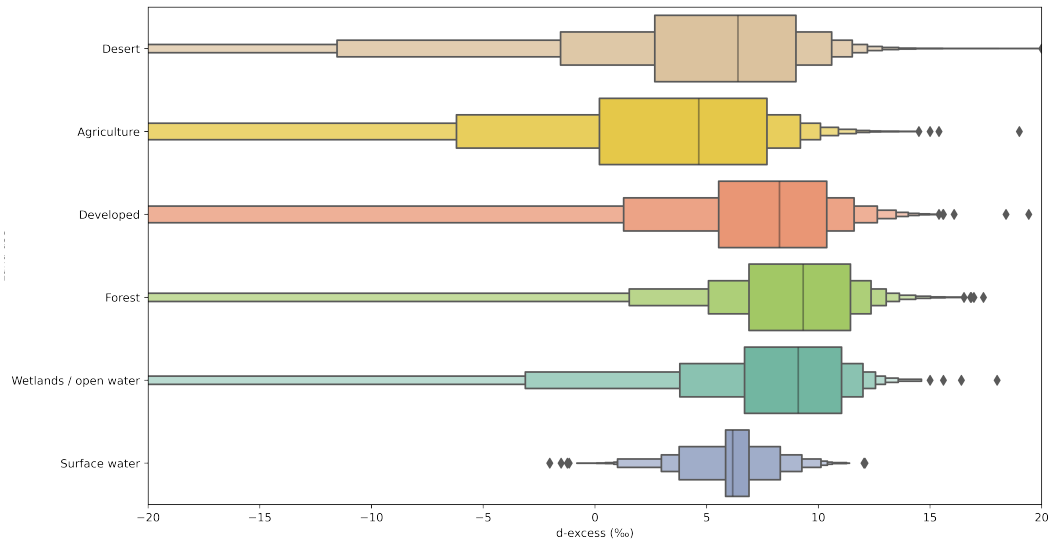


Figure 7. Distributions of groundwater d grouped by the dominant land type from NLCD ? in the HUC12 ? of the observation. The data are displayed as letter-plots ?, where the central line is the data median, the innermost box contains 50% of the data, the remaining boxes each contain 50% of the remaining data, and thus a diminishing proportion of the total data (i.e., 25%, 12.5%, 6.25%, etc). The black diamonds represent outliers. The plot contain between 85 and 95% of the data available for each land type and thus reasonably represents the distribution of d associated with groundwater from each land use type, even though samples with very low d are not shown. The desert land class includes barren land (often playas or dried lakebeds), shrub/scrub, grasslands/herbaceous. The agricultural land class includes pasture/hay and cultivated crops. The developed land class includes developed land of any intensity. Forest includes evergreen, deciduous and mixed forest. The wetlands/open water land class category any type of wetland as well as open water. The distribution of our 4303 river samples is also shown for context.

3.3.2 Isotopic signals of evaporation at low elevations suggests contributions of irrigation return flows to streamflow

530

Greater spatial and temporal variability in both $\delta^{18}O_{diff}$ and d_{diff} in lower elevation, higher stream order, arid reaches suggests the importance of various spatially and temporally heterogeneous processes and water sources that may alter streamflow isotope ratios relative to upstream values. Positive values of $\delta^{18}O_{diff}$ and negative values of d_{diff} in more arid regions of each basin suggests that evaporated waters compose a non-trivial fraction of streamflow in these areas (Figures 5, 6, S9 and S10), especially in the later part of the growing season (Figure 9) when streams depend more heavily on groundwater fluxes. We observed isotopic evidence of contributions of evaporated waters to rivers in all basins (Figure 6), though it was most apparent in Lower Colorado River Basin, lower elevation regions of the Upper Colorado River Basin, California's Central Valley, near Great Salt Lake in the Great Basin and throughout the Snake River Plain (Figures 5 and S9).

535

540

The isotope ratios and d we observe in low elevation, high stream order arid reaches are similar to those we would expect to observe in highly evaporative contexts, like within lakes, intermittent flow rivers, or downstream of wetlands. Yet the majority of rivers in our study are perennial, and most are not characterized by substantial wetlands. The evapoconcentration in our dataset is unlikely to arise from river or reservoir evaporation because both evaporation of reservoirs and evaporation to inflow ratios in the region tend to be low, especially for deep man-made reservoirs. Instead, isotopic evidence of evapoconcentration occurs in waterways likely to be affected by anthropogenic hydrologic alteration and characterized by larger fractions of 'young water'.

545

555

We tested the hypothesis that the spatial pattern of isotopically-inferred evaporation could arise from contributions of irrigation return flows to streams and reservoir releases. Within each basin, on average, d_{diff} was most negative, indicating isotopic evidence of evaporation, at sites with the highest proportion of total inflows attributed to agricultural return flows and highest at sites with no apparent contributions of agricultural return flows (Figure 8). Reservoir influence was associated with low d_{diff} more often where dams are used for water management and water supply (e.g., Upper Colorado, Lower Colorado, Great Basin, and California) and were associated with high d_{diff} in the Pacific Northwest, where dams are more often used for hydropower. Intermittent streams and canals in arid regions were sometimes associated with low d_{diff} as well, even when no water was contributed by agricultural irrigation.

560

We demonstrated the relationships of agricultural and reservoir influence on d_{diff} statistically in a linear mixed effects model (Table 3). The fraction of streamflow estimated to come from agricultural irrigation return flows and a categorical variable delineating reservoir influence together explained 8.0% of the variance in d_{diff} , with the whole model (including random group effects) explaining 14.3% of the variance in the dataset. Both explanatory variables were significant ($p < 0.01$), and, as expected, exhibited negative slopes indicating that greater agriculture and reservoir influences tended to produce lower ~~more evapoconcentrated~~ d_{diff} values, indicative of evaporative effects. When we included the ratio of actual evaporation to precipitation with these explanatory variables, all three

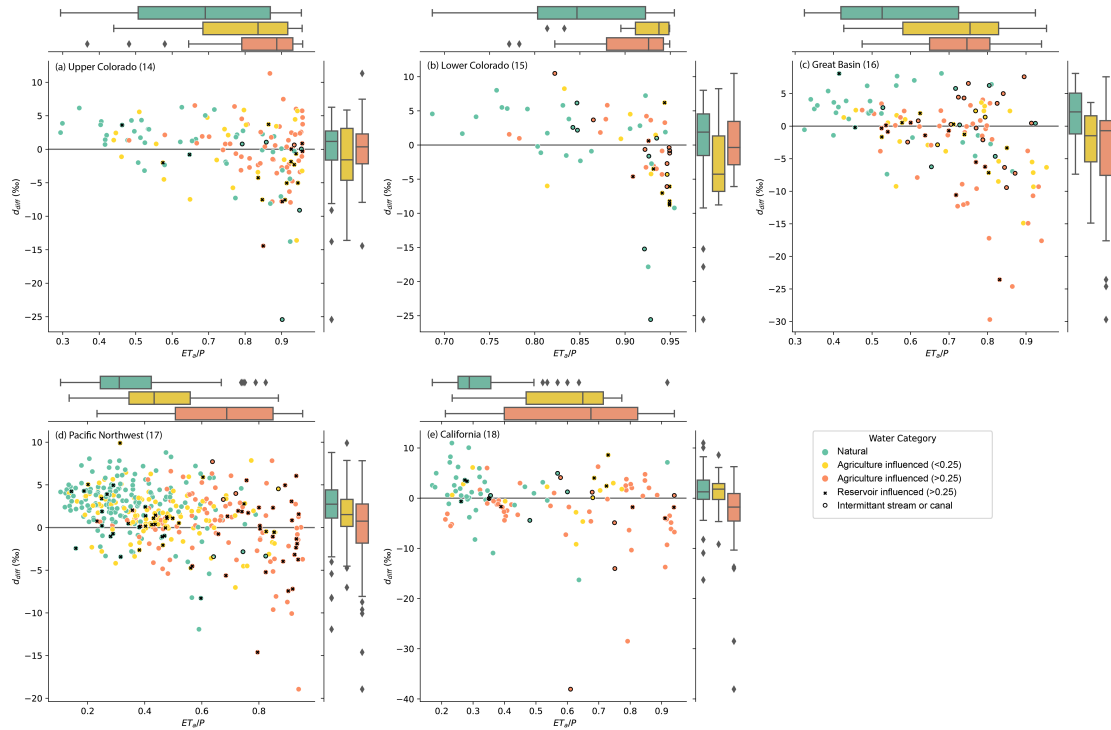


Figure 8. Relationship of aridity to d_{diff} , by water use categories and basins. Natural waters are not estimated to be influenced by agricultural irrigation. Fractions of agricultural irrigation contributing to streamflow are estimated using water use data and land cover data and do not account for losses to evapotranspiration. We identified reaches affected by large reservoirs and reaches categorized as intermittent or as canals or ditches with additional symbology.

are significant ($p < 0.01$) and explain 15.2% of the variance through fixed effects, and 23.0% of the variance overall (fixed and random effects). Among the linear mixed effects models tested, it exhibited the highest log likelihood value, explained the greatest amount of variance using fixed effects, and reduced the amount of variance attributed to random within-basin effects.

While this statistical model performance is not substantially better at explaining variance in d_{diff} than the model that uses aridity alone, the findings do suggest that both agricultural activity and reservoirs influence the isotope ratios of streamflows across the Western US. The low variance explained by these models is expected, due to the difficulty estimating true long term mean agricultural return flux with the spatial and temporal resolution of the available data, the confounding influences of season and year on the response variable, the potential for isotopically heterogeneous reservoir effects, the covariance of both irrigation return flows and the presence of reservoirs with aridity and elevation, and the spatially variable effect of irrigation on streamflows ?. [The statistical linkage between irrigation water use and the isotopic response would likely be improved by taking a time-variable approach to](#)

Statistical model	β (\pm s.e.)	I (\pm s.e.)	HUC2 (group)	Cond. R ²	Fixed R ²	Log like- lihood
$d_{diff} \sim Elev + I$	<i>Elev</i> : 0.001 (0.00)*	-1.93 (1.01)	4.33	20.9%	4.4%	-2254
$d_{diff} \sim \frac{ET}{P} + I$	$\frac{ET}{P}$: -7.85 (0.77)*	4.86 (1.08)*	4.37	30.2%	13.9%	-2209
$d_{diff} \sim F_{irr} + Res + I$	<i>F_{irr}</i> : -3.49 (0.48)* <i>Res</i> : -1.75 (0.45)*	0.95 (0.59)	1.43	14.3%	8.0%	-2224
$d_{diff} \sim \frac{ET}{P} + F_{irr} + I$	$\frac{ET}{P}$: -6.50 (0.88)* <i>F_{irr}</i> : -1.60 (0.54)*	4.39 (0.83)*	1.941	22.8%	14.8%	-2204
$d_{diff} \sim \frac{ET}{P} + F_{irr} + Res + I$	$\frac{ET}{P}$: -6.08 (0.88)* <i>F_{irr}</i> : -1.67 (0.54)* <i>Res</i> : -1.22 (0.44)*	4.32 (0.82)*	1.861	23.0%	15.2%	-2200

Table 3. Results of linear mixed effects models with 764 observations and 5 groups. The minimum and maximum group sizes were 48 and 387, respectively. The models do not include any samples from reaches characterized as an intermittent stream or canal or where NWM indicates that the maximum streamflow is 0 m³ s⁻¹. Random effects apply only to the intercepts. An asterisk indicates that a regression coefficient is statistically significant at p<0.01. Conditional R², which gives the total model variance explained, are reported alongside the fixed R², which gives the variance explained by fixed effects (i.e., explanatory variables) and the log-likelihood, which can be used to evaluate the relative performance of different models.

575 [estimating river isotope ratios, and the contribution of irrigation water in the river, which may be doable with](#)
[improvement to both precipitation isotope datasets and higher spatial and temporal resolution irrigation water use](#)
[datasets \(e.g., ?\).](#)

3.4 ~~Seasonal patterns in observation-model differences support~~ [Further evidence supporting](#) irrigation contributions to streamflow

580 [We have statistically quantified isotopic evidence for irrigation contributions to streamflow. However, the statistical](#)
[model performance is not substantially better at explaining variance in \$d_{diff}\$ than the model that uses aridity](#)
[alone. To further investigate our findings, we include analyses of additional lines of evidence. We evaluate signals](#)
[embedded in seasonal patterns in our dataset, as well other studies, spatial variability in groundwater isotope ratios,](#)
[and evaluation of the NWM with a well level relative to river level dataset.](#)

585 3.4.1 [Seasonal patterns in observation-model differences](#)

There are systematic patterns in $\delta^{18}O_{diff}$ and d_{diff} when examined across the growing season that support our spatial assessment of the contributions of irrigation to streamflow. For example, $\delta^{18}O_{diff}$ tends to be greater during the latter months of the growing season relative to the mean $\delta^{18}O_{diff}$ value for the month of June for that site and year (Figure 9a) in most basins and months. The pattern is especially evident in the Great Basin and California.

590 Likewise, d_{diff} is lower in July, August, September relative to June (Figure 9b), in the Great Basin and California. The contrast between basins with both increased $\delta^{18}O_{diff}$ and decreased d_{diff} (Great Basin and California) and those with only increased $\delta^{18}O_{diff}$ and little change in d_{diff} (Upper and Lower Colorado and Pacific Northwest) suggests that two different mechanisms may drive isotopic change during the growing season.

595 In California and the Great Basin, which are characterized by $\delta^{18}O_{diff}$ increases and d_{diff} decreases over the growing season relative to June, we suggest increased contributions of evaporated waters to rivers later in the growing season. In California, this may reflect the water use and irrigation return flows contributing to streamflow in the Central Valley.

600 In the Upper and Lower Colorado and Pacific Northwest, where we observe small $\delta^{18}O_{diff}$ increases and little d_{diff} change relative to June, we suggest sustained dependence on groundwater discharge from high elevations to streamflow during the growing season ????. In downstream sections of the Upper Colorado and the Lower Colorado, where rivers are characterized by discharges from large reservoirs, the seasonal invariance may reflect that the primary ‘water source’ regions for these reaches are reservoirs, which retain snowmelt from early in the season and discharge it later in the season.

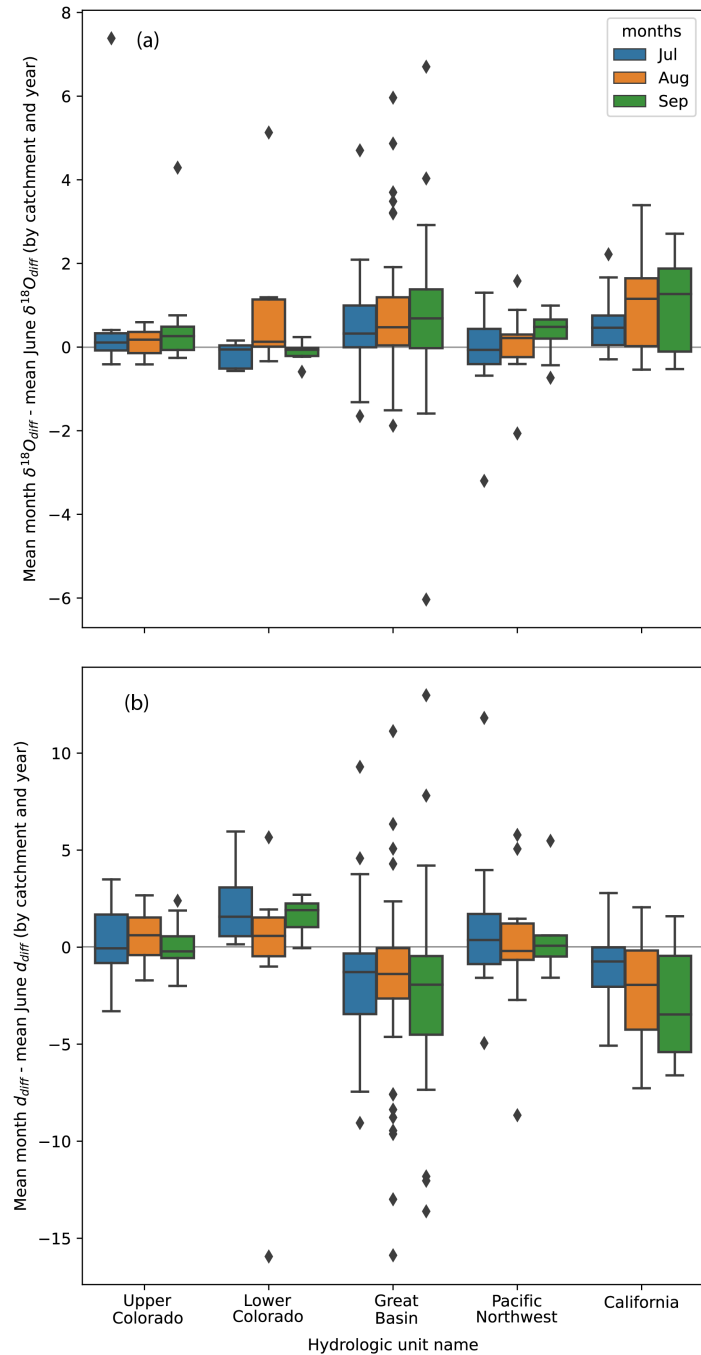


Figure 9. Evaluation of seasonal variability in observation-model comparisons. Data include all reaches and years with collections in the month of June as well as 2 of the 3 other months of the summer season. (a) The distribution (represented by boxplots) of month-specific differences from June $\delta^{18}O_{diff}$ by basin. (b) The distribution (represented by boxplots) of month-specific differences from June d_{diff} . The boxplots show the median, 25th and 75th percentiles as the box, whiskers extend to points that lie within 1.5 IQRs of the lower and upper quartile, and observations that fall outside this range are displayed as diamonds.

3.4.2 Literature and other datasets~~support isotopic inference of irrigation return flows contributing to streamflow~~

605

Numerous prior studies have investigated the influence of irrigation on streamflow. Estimates suggest that, depending on the irrigation type, as much as 50% of applied water may recharge groundwater and/or arrive at surface waters through shallow groundwater infiltration and subsequent discharge to streams ?. Likewise, irrigation has been demonstrated to increase streamflows during low flow periods ??, if the applied water comes from surface water diversions.

610

Local contributions of groundwater to streams from irrigation-based recharge are supported by the d values of groundwater in agricultural regions. Groundwater from regions influenced by agricultural irrigation exhibited lower mean d relative to deserts, including dried terminal lakes and playas, developed areas which may include turf grass irrigation, forested regions, wetlands or open waters and surface waters (Figure 7). Based on the isotope ratios of groundwater in irrigated areas and prior isotopic inference ?, we hypothesize that inclusion of irrigation-recharged groundwater discharge as a source of water to streams in NWM would decrease the difference between modeled and observed isotope ratios in our dataset.

615

The isotopic inference that irrigation return flows are an important missing process in the NWM is supported by an independent statistical comparison of the NWM groundwater discharge with the ? dataset and the agricultural water use data. The ? data is the fraction of well water levels that lie below the proximal river water level in a catchment and provides some idea-estimate of hydraulic head and direction of groundwater-surfacewater exchange. When the fraction is high, the river (under correct permeability conditions) would be expected to lose water to groundwater, whereas when the fraction is low the river would be expected to gain water from groundwater discharge.

620

We hypothesize that if NWM accurately represents groundwater discharge to streams, the ? well water level comparison to stream water level dataset should be able to predict the summer mean NWM groundwater discharge flux with a large proportion of variance explained. However, the ? data weakly ($R^2 = 0.028$, $p < 0.01$) predict the NWM groundwater discharge rates in a simple linear regression. The regression relationship between the variables is negative, as expected, where river reaches with a greater proportion of their well water levels above proximal river water levels correspond to reaches with greater groundwater discharge fluxes (Figure S11). Though the regression is significant, it has almost no predictive capacity, contrary to what we expectexpectations.

625

630

The weakness of the statistical relationship between the ? dataset and the NWM groundwater discharge flux may be related to shallow aquifers, which are not considered by NWM, and/or agricultural irrigation, as well as the water source (surface or ground water) used for that irrigation (Figure S12). We did not assess the potential for NWM groundwater discharge to reflect the presence of shallow aquifers. However, we observe that the influence of irrigation on groundwater levels is non-stationary, depending on both the groundwater discharge magnitude as well as the source of irrigation water. For this reason the relationship is difficult to assess statistically. In river reaches where NWM indicates little groundwater discharge (0^{th} to 20^{th} percentile qBucket), irrigation sourced from surface

635

water is associated with a smaller fraction of well water levels below river level (smaller y value in Figure S12) than those without irrigation. Conversely, in river reaches with substantial groundwater discharge (80th to 100th percentile qBucket), agricultural irrigation with water from either surface or groundwater tends to be associated with a larger fraction of well water levels below river level (larger y value in figure S12) compared to reaches without any agricultural irrigation. Based on these patterns we suggest that in dry areas, irrigation from surface water appears to contribute to groundwater recharge, whereas in wet areas, irrigation appears to contribute to decreased water table elevations. At all groundwater discharge percentiles, surface water irrigation contributes to higher water tables, whereas irrigation from groundwater contributes to lower water tables.

Some part of this signal is regional. Reaches from more arid basins compose a greater proportion of the lower percentile qBucket reaches, and reaches from humid or seasonally snowy basins compose a greater proportion of the higher percentile qBucket reaches. However, when evaluated by basin, the relationships are similar. The finding is consistent with modeling studies, which showed lower stream discharge when irrigation water came from groundwater, and greater stream discharge when irrigation water came from surface water. Our analysis suggests that agricultural irrigation is likely to influence groundwater levels and groundwater discharge on a landscape scale and produces gaining streams and contributes to streamflow in otherwise arid, losing reaches of rivers.

3.5 Implications of including irrigation return flows into NWM calculations

Our evaluation of the NWM-driven isotope mass balance calculations suggest that the NWM accuracy would be improved by including agricultural return flows in the water sources sustaining streamflow in the NWM. In effect, agricultural return flows are simply groundwater fluxes to streams that occur at lower elevations than the majority of the groundwater discharge sustaining streams. Based on magnitudes of d_{diff} , these lower elevation groundwater fluxes can sometimes be large. Because the NWM is calibrated to actual streamflows which contain these return flows, these fluxes are currently being misallocated in the model. Inaccuracies in any model terms or fluxes influence the model's capacity to project accurate streamflows, particularly under non-stationary hydrologic conditions. Accurate model water source inclusion, particularly at low elevations where water use and availability is most critical, thus has implications for the model's utility to stakeholders, including water managers and users.

Under current conditions, agricultural return flows may be critical for sustaining streamflow late in the growing season (August or September) or during drought periods. Sustained streamflow in certain reaches is critical for 1) water access for surface water diversions and 2) water availability for species' use. For example, protected fish species survival requires that waterways meet thresholds of water quality, temperature, and depth for survival. Water managers make decisions about water allocations and reservoir releases in part to meet these habitat needs. Agricultural return flows have the capacity to help sustain streamflow, but with potentially negative effects on water quality, through agriculture-associated salinization, increased concentrations of nitrate, and other nutrients, contributions of pesticide and fertilizers, or alterations to water temperature profiles. These contributions of agricultural waters contribute to sustaining flow but threaten water availability. Thus, inclusion of groundwater

return flows from irrigation to rivers in the Western US supports improved assessments of water availability both through improved modeling of streamflows and enhanced ability to model water quality.

675 Explicit inclusion of irrigation return flows will assist the NWM in better projecting streamflows during periods of hydrologic non-stationarity, as are likely to characterize the hydroclimatic elements of climate change. Non-stationary processes include hydrologic changes arising from the ongoing mega-drought of the southwestern US ?, associated changes in water use for irrigation ?, intense precipitation events like monsoons or major storm events that are observed to be increasing in intensity with climate change ??, and projected changes to future snowpack depth and melt timing ??. The ongoing aridification of the southwestern US is characterized by increased evapotranspiration ?,
680 and changes to groundwater recharge and discharge associated with decreases in snowpack and changes to snowpack melt patterns ?. Understanding the groundwater flux contributions of areas with shallow water tables to streamflow during major precipitation events will help better characterize areas at risk for flooding and inform appropriate water management strategies.

4 Conclusions

685 The isotope mass balance evaluation of the NWM revealed similarities between the isotope mass balance estimated isotope ratios (modeled) and observed isotope ratios. The mass balance approach represented as much as 75% of the variance in the observations, depending on the water isotopologue evaluated. This suggests that, on [meanaverage](#), during the summer, the NWM correctly represents the relative proportions of groundwater and surface runoff fluxes sustaining streamflow, and the gridded isotope datasets are appropriate for the analysis.

690 The observation-model differences exhibited spatial and seasonal structure, suggesting that the NWM is missing important additional water sources that contribute to streamflow. Specifically, the observation-model differences that plot above the equilibrium line (Figure 2) suggest the importance of direct contributions of snowmelt to streamflow in humid areas. Those that plot below the equilibrium line suggest the importance of groundwater sources characterized by evaporation in arid areas. We tested the hypothesis that agricultural irrigation return flows
695 are the missing evaporated water source in arid regions, and found them to be a significant predictor of observation-model differences. [This Future work may benefit from taking a time-varying approach to estimation of streamflows and agricultural contributions to streams, as the difference in timescale between the observations and models is a source of uncertainty. Nonetheless, our](#) finding is supported by multiple lines of evidence including the [seasonality of observation-model differences](#), relationship of land use to isotopic signals (d) of evaporation in groundwaters,
700 a comparison of NWM groundwater discharge with an independent assessment of the potential for groundwater discharge and isotopic and modeling study conclusions from the literature.

Our findings suggest that the NWM accuracy would be improved by including agricultural irrigation fluxes into the NWM water sources. Agricultural irrigation recharged groundwater functions as lower elevation baseflow fluxes, and are likely to be critical for sustaining streamflow during drought periods or late in the growing season. Inclusion

705 of this specific source into groundwater fluxes would improve the ability to meet water manager and water user NWM
data needs. Specifically, water managers use predictions of reach-specific flows at lower elevations during summer
precipitation events and monsoons to assess flood risk, or to inform dam releases (if dam releases are incorporated into
the NWM) to assess the volume of water required to achieve specific management goals like fish species preservation
or dam water level maintenance for hydropower production. Likewise, explicit inclusion of irrigation return flows
710 in NWM calculations will assist in accurately predicting and projecting streamflows in heavily managed sections
of river in the event of changing irrigation practices, increased evapotranspiration, or water supply reductions and
fallowing of agricultural fields, which would change or halt irrigation groundwater fluxes. Finally, our findings have
implications for areas at risk for diminished water availability due to issues of quality, arising from the entrainment
of fertilizer and pesticides and as well as dissolution and delivery of salts.

715 *Data availability.* Data are publicly available ?.

Author contributions. Conceptualization and funding acquisition: ALP and OLM; Data curation: PCL, MCM, MK, JR,
and JRB; Methodology, investigation and formal analysis: ALP and PCL; Project administration and supervision: ALP;
Visualization: ALP; writing (original draft): ALP; Writing - review: OLM, PCL, MCM, JR, MK and JRB

Competing interests. The authors declare no competing interests

720 *Acknowledgements.* The authors acknowledge financial support from the US Geological Survey (USGS) Water Mission area
Water Quality Processes Division. We appreciate comments from two USGS peer reviewers, whose comments improved the
quality of the manuscript. The views expressed in this article are those of the author(s) and do not necessarily represent the
views or the policies of the US Environmental Protection Agency. Any use of trade, firm, or product names is for descriptive
purposes only and does not imply endorsement by the US Government.

